Earthquakes and Structures, *Vol. 8, No. 3 (2015) 681-697*
DOI: http://dx.doi.org/10.12989/eas.2015.8.3.681

Seismic hazard assessment for two cities in Eastern Iran

Alireza Farzampour* and Arash Kamali-Asl[a]

Department of Civil Engineering, Sharif University of Technology, Tehran, Iran

(Received April 23, 2014, Revised December 8, 2014, Accepted December 14, 2014)

Abstract. Iran as one of the countries located on the Alpine-Himalayan seismic belt has recently experienced a few number of catastrophic earthquakes. A well-known index of how buildings are affected by earthquakes is through assessment of probable Peak Ground Acceleration (PGA) and structures' response spectra. In this research, active faults around Kerman and Birjand, two major cities in eastern parts of Iran, have been considered. Seismic catalogues are gathered to categorize effects of surrounding faults on seismicity of the region. These catalogues were further refined with respect to time and space based on Knopoff-Gardner algorithm in order to increase statistical independency of events. Probabilistic Seismic Hazard Analysis (PSHA) has been estimated for each of cities regarding 50, 100, 200 and 500 years of structures' effective life-span. These results subsequently have been compared with Deterministic Seismic Hazard Analysis (DSHA). It has been observed that DSHA not necessarily suggests upper bound of PSHA results. Furthermore, based on spectral Ground Motion Prediction Equations (GMPEs), Uniform Hazard Spectra (UHS) and spectral acceleration were provided for 2% and 10% levels of probability of exceedance. The results show that increasing source-to-site distance leads to spectral acceleration reduction regarding each fault. In addition, the spectral acceleration rate of variation would increase if the source-to-site distance decreases.

Keywords: seismic hazard analysis; response spectra; uniform hazard curves; life-span effect; eastern Iran

1. Introduction

Earthquakes cause losses and damages to a number of people every year. Iran as one of the most vulnerable countries located on Alpine-Himalayan seismic belt has experienced a number of events in the last century. Fig. 1 shows the density of these events in Iran for the recent 50 years (Tavakoli and Ghafory-Ashtiany 1999). The most intense seismic responses to the general drift of Arabian plate toward Eurasia plate have happened in eastern zones of this country.

Occurrence of significant events in history of this region, like Silakhor (with Mw 7.4), Salmas (with Mw 7.4), Tabas (with Mw 7.7), Bam (with Mw 6.6) and Saravan (with Mw 7.7) have shown the high seismicity of Iran. Table 1 demonstrates some major events occurred in past history of Iran.

Additionally, a number of researches were allocated to investigate GMPEs for various parts of

*Corresponding author, Graduate Student, E-mail: alirezafarzampour4230@gmail.com
[a]Graduate Student, E-mail: arashkamaly69@gmail.com

http://www.techno-press.org/?journal=eas&subpage=7 ISSN: 2092-7614 (Print), 2092-7622 (Online)

Iran (Motaghi and Ghods 2012, Saffari *et al*. 2012, Zare *et al*. 2008). In this regard, Mousavi *et al*. (2012) investigated a set of candidate ground motions in the Zagros region of Iran according to regional, local and NGA models, resulting in better consistency of local models with recorded data. However, Shoja-Taheri *et al.* (2010) indicated that NGA models may confidently be applied with Iranian plateau, suggesting combination of NGA models and Iranian databases as a useful approach for new GMPE derivation. Alavi *et al.* (2011) have derived new models by implementation of multi expression programing method for assessment of the time-domain ground-motion parameters of PGA, PGV and PGD. In addition, Ghodrati Amiri *et al.* (2007) proposed the GMPEs for PGA, PGV, and EPA parameters for areas within the seismic zones of Zagros, Alborz and Central Iran with rock and soil substructures.

The higher density of events on the south-west and central-east of Iran necessitates the need for further investigation of these regions according to soil and structures' seismic behavior. For the last 100 years there are at least 18 catastrophic earthquakes reported in Iran, among which Bam earthquake as one of the recent most destructive events (with M_w 6.5) caused notable number of deaths, although the magnitude of this earthquake was not significant (Zare and Hamzehloo 2004). In addition, the Ancient Citadel of Bam city was destroyed drastically after Bam earthquake due to poor construction materials.

Cauzzi and Faccioli (2008) have suggested a new set of empirical equations for prediction of displacement response spectra. Vacareanu *et al.* (2014) have proposed empirical GMPEs to improve previous generation of ground motion prediction models for Romania and provide 300 km distance range of applicability. A number of studies conducted to investigate the probable PGA and seismicity for distinctive parts of Iran (Abdollahzadeh *et al.* 2013, Berberian 1981, Berberian *et al.* 1984, Ghodrati Amiri *et al.* 2003, Raschke 2013, Tavakoli 2002, Engdahl *et al*. 2006, Mirzaei *et al*. 1999), and especially in east of Iran (Berberian 1979, Berberian 1982, Berberian *et al.* 1999, Berberian *et al*. 2000, Walker *et al.* 2009). In addition, to evaluate the structures' spectral behavior in different parts of Iran, Hosseinzadeh (2008) evaluated UHS for Bam city for return periods of 475 and 2475 years. Ghasemi *et al.* (2009) developed a new ground-motion prediction equation for 5%-damped horizontal spectral acceleration for Iran using selected West-Eurasian records; Rahgozar *et al.* (2012) produced UHS for different hazard levels for Bojnurd city in Iran.

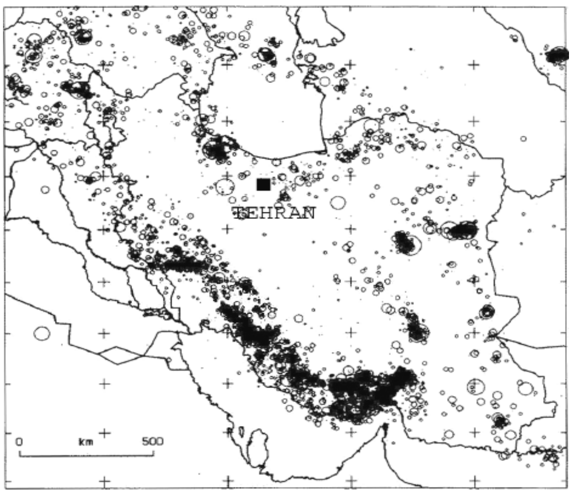

Fig. 1 The epicenter of recent events in Iran (Tavakoli and Ghafory-Ashtiany 1999)

Table 1 The most destructive earthquakes in Iran (Tavakoli and Ghafory-Ashtiany 1999, Bartels and VanRooyen 2012)

No.	Year	Location	Magnitude	Mortality (dead)
1	1909	Silakhor	7.4	8000
2	1930	Salmas	7.4	2500
3	1953	Torud	6.4	200
4	1960	Lar	6.7	400
5	1962	Buyin	7.2	10,000
6	1968	Dasht-e-Bayaz	7.4	10,500
7	1972	Qir	6.9	4000
8	1977	Khorgu	7	150
9	1978	Tabas	7.7	600
10	1979	Qayen	7.1	130
11	1990	Rudbar-Manjil	7.2	35,000
12	1997	Ardebil	6.1	1100
13	1997	Birjand	7.3	1500
14	1997	Ghaen	7.3	1500
15	2003	Bam	6.5	40,000
16	2005	Zarand	6.4	600
17	2012	Ahar-Varazaghan-Heris	6.4	300
18	2013	Saravan	7.7	40

Kerman as one of the most historical and populated regions located in east of Iran has experienced severe earthquakes during last decades. Generally, structures constructed in this region are not built according to seismic standards. Most of them are made from mud prone to serious damages (Bilham 2009). South Khorasan as another vulnerable region (Walker *et al.* 2004a, b, Walker and Khatib 2006) has suffered much as well, due to at least 3 destructive events during last 50 years. From which Birjand city, the capital of the stated region, once has experienced an earthquake with moment magnitude of 7.3, causing 1500 deaths.

In this research, Birjand and Kerman cities were chosen as two tectonically-active poorly-constructed areas of east of Iran for Seismic Hazard Analysis (SHA). To estimate probable PGA based on Campbell (1981), Sadigh *et al.* (1986) GMPEs, the 50, 100, 200 and 500 years of life-span are investigated. The UHS and spectral acceleration curves were developed according to 2% and 10% probability of exceedance based on Ghodrati Amiri *et al.* (2009), Sadeghi *et al.* (2010) spectral GMPEs, respectively. Accordingly, five major active faults located in eastern region of Iran for two adjacent provinces have been studied. For this area, the major active faults are Kuhbanan, Golbaf, Esfandiar, Dasht-e-Bayaz and Nehbandan-e-Sharqi.

2. Seismotectonic

Active faults along Alpine-Himalayan seismic belt could be considered as the main characteristic of the Iranian plateau. This plateau is a “constrained convergent zone” surrounded by

Arabian plate in the west and the Indo-Australian plate in the east (Berberian 1981). Eastern regions of Iran have experienced a number of catastrophic events during last decades (Tavakoli and Ghafory-Ashtiany 1999). South eastern part of the Iranian plate collided with oceanic crust in Makran area (Regard *et al.* 2010), the surrounding plates of this area grind roughly from north east and they often remain wedged against each other for long periods before a sudden movement. In addition, eastern areas could be affected by Arabian and Indo-Australian interaction from different orientations leading to right-lateral shear; therefore, eastern parts may possibly experience a significant density of events with considerable intensity (Walker and Jackson 2004b).

2.1 Kuhbanan

The Kuhbanan fault with a strike-slip reverse-component motion (Shafiei Bafti 2009) with the extent of 300 km is located between Tabas and Yazd blocks in the south east of Central Iran micro-plate, from the north west of Kerman to the east of Bafgh (Koreie 2005). The Kuhbanan fault has been associated with three major earthquakes in the 20th century. The earthquake with moment magnitude of 6.4 has happened on the 22 February 2005 ruptured 10 km of this fault.

Movement in the south east and central segments has been dextral strike-slip with a large reverse component, and in the north western segments has been dextral strike-slip with a large normal component (Koreie 2005).

2.2 Dasht-e-Bayaz

Dasht-e-Bayaz is a left-lateral strike-slip fault with 200 km length, located in north eastern part of the Iran and north of the Birjand city. The earthquakes of Dasht-e-Bayaz and Khuli-Buniabad with 7.1 moments of magnitude, occurred in 31 August 1968 and 27 November of 1979 are associated with this fault. Distributed strike-slip faulting is widespread in the region and there are indications that the Dasht-e-Bayaz fault is evolving from several coalescing short faults (Walker *et al.* 2004a).

2.3 Golbaf

Golbaf is an oblique reverse mechanism fault with the length of 180 km (Berberian and Qorashi 1994) extending from the southern end of the Nayband fault in the north to the Jebel-e-Barez Mountains in the south, to the northern part of the Gowk fault. The Golbaf fault is a part of the Nayband-Golbaf-Sabzevaran fault system, located in west of the Lut block. There are at least five catastrophic earthquakes occurred in the past thirty years according to this fault. The earthquakes of 11 June 1981 with M_w 6.6 and that of 28 July 1981 with M_w 7.1 are attributed to the Golbaf fault (Shokri *et al.* 2011).

2.4 Esfandiar

Esfandiar is a reverse fault with the length of 230 km, stretching from Tabas in north to Nayband fault in south. This fault located in east-central of Iran. The earthquake of 11 May 1973 with body magnitude of 5.1 is amongst the significant events attributed to this fault (Berberian 1981).

Table 2 Active faults in eastern of Iran

Earthquake	Type	M_{max}	M_{min}	Events (K-G Refined)
Kuhbanan	Strike-slip	7.2	4	65
Golbaf	Reverse	8.1	4	38
Esfandiar	Reverse	8.4	4	40
Nehbandan-e-Sharqi	Reverse	8.3	4	34
Dasht-e-Bayaz	Strike-slip	8.1	4	139

2.5 Nehbandan-e-Sharqi

The Nehbandan fault with the length of 200 km is one of the major longitudinal faults in the east of Iran, extending from the Nosratabad area to the Sefidabeh city. The earthquake of 8 March 1928 with body magnitude of 5.2 is attributed to this fault. The East and West Nehbandan faults are two sub-parallel faults, 10 to 20 km apart. Although segmented, they both have a total length of 200 km. To the south, they end near Nosratabad city and they appear to link southward with the Kahurak and Nosratabad faults. To the north, the Nehbandan faults enter a zone of several strike-slip and thrust faults that include the Birjand, Purang, Gazik and Avaz fault systems (Walker and Jackson 2004b).

3. Seismicity

Events could be categorized into two groups, the historical earthquakes (before 1900), and the instrumentally recorded earthquakes (after 1900). In this study, events occurred for the last 110 years in a radius of 100 km from both cities have been investigated. More than 300 catalogues were collected. The catalogues were gathered from the reporting agency (IIEES). Independency of events should be considered for stationary Poisson process. In this regard, the data were refined regarding time and space based on Knopoff-Gardner method (Gardner and Knopoff 1973) in order to filter the main shocks from foreshocks and aftershocks.

From the total of 15000 events, 1360 independent and declustered events were selected. These main shocks were filtered with respect to distance and time of occurrence. Moreover, the implemented catalogues have different magnitude scales, since they were announced by different procedures, all the magnitude scales of the catalogues were changed to M_w as a representative of event’s magnitude. The type and characteristics of each fault along with maximum magnitude of events were estimated (Kijko 2004) in Table 2. In this study, two distinctive sites have been considered for Seismic Hazard Analysis (SHA) as shown in Fig. 2. In addition, the characteristics of soil condition at the studied sites were investigated by IIEES reports and assumed as rock type for further implementation in GMPEs.

4. Deterministic approach

DSHA involves the development of the particular seismic situation including the postulated occurrence of an earthquake in a specified location (Kramer 1996). In this study, Sadigh and

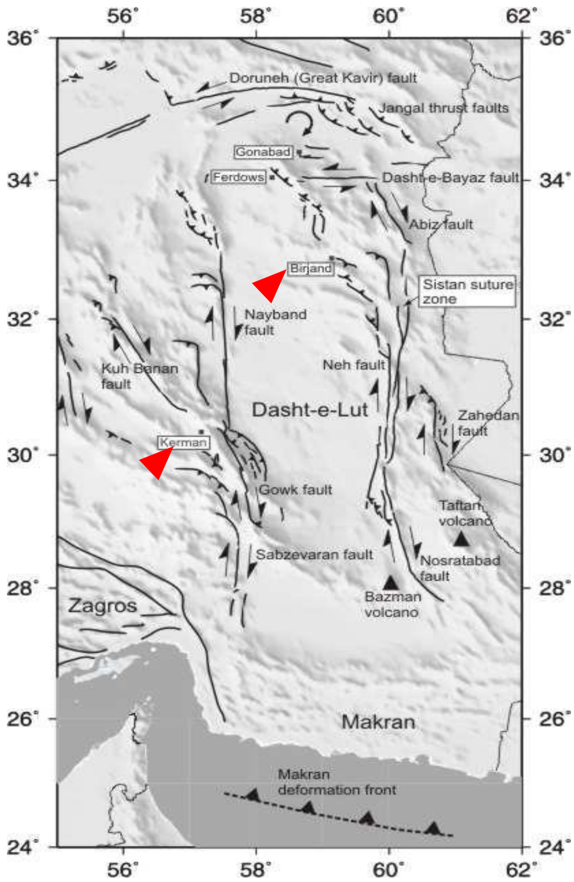

Fig. 2 Two investigated cities and potential seismogenic sources

Campbell GMPEs were used to estimate PGA. Additionally, in order to evaluate the relationship between fault characteristics and wave-surface magnitude, two formulas (Eqs. (1) and (2)) have been implemented:

- Nowruzi (1985)

$$Ms = 1.239 + 1.244 \log L \tag{1}$$

where L is the length of the fault; and Ms is the wave-surface magnitude, and:

- Wells and Coppersmith (1994)

$$Ms = a + b \log(SRL) \tag{2}$$

where SRL is surface rupture length. a and b are fault mechanism parameters. For instance, in reverse faults these parameters are 5 and 1.22, respectively.

The faults were categorized into area and line seismogenic sources based on the distribution of events. If the events allocated to each fault are widespread enough, the fault could be assumed as an area fault, whereas the line source is a fault with more focused distribution of events. In this study, the Kuhbanan, Golbaf, and Dasht-e-Bayaz faults are assumed as area sources and the Esfandiar and Nehbandan-e-Sharqi are defined as line sources. The DSHA method results are

Table 3a Results of deterministic method

Source (Kerman)	R (km)	SRL	M	PGA(g) [Campbell]	PGA(g) [Sadigh]
Kuhbanan	35.5	79	7.44	0.15	0.16
Golbaf	40.2	99	7.15	0.11	0.12
Esfandiar	380	37	7.04	0.0041	0.0023
Nehbandan-e-Sharqi	540	47	7.28	0.0031	0.0017
Dasht-e-Bayaz	450	88.5	7.37	0.0047	0.0026

Table 3b Results of deterministic method

Source (Birjand)	R (km)	SRL	M	PGA(g) [Campbell]	PGA(g) [Sadigh]
Kuhbanan	415	79	7.44	0.0058	0.0033
Golbaf	475	99	7.15	0.0033	0.0019
Esfandiar	141.7	37	7.04	0.02	0.016
Nehbandan-e-Sharqi	12.7	47	7.28	0.29	0.35
Dasht-e-Bayaz	16.4	88.5	7.37	0.27	0.31

indicated in Tables 3a and 3b. This approach has been summarized with three general steps according to Reiter (1990):

- Recognition of the events: all the node, line and area seismogenic sources in the vicinity of the site should be detected; in other words, the magnitude and the source-to-site distance of the events for each seismogenic source should be gathered.
- Determination of the maximum considered earthquake: the MCE should be distinguished, and for each source a pair of (M, R) would be produced.
- GMPE selection: GMPEs are selected in order to estimate the PGA (Eq. (3)) for each representative of (M, R).

$$a = F(M, R) \tag{3}$$

DSHA provides a straightforward framework for evaluation of worst-case ground motions. However, it does not consider any information on the likelihood of an earthquake occurrence as well as the effects of uncertainties in the various steps required to compute the resulting ground motion characteristics (Kramer 1996).

5. Probabilistic hazard analysis

5.1 Gutenberg-Richter law

For estimation of the probable PGA, after catalogue refinement, events were sorted according to the number of events with more than a certain magnitude. The occurrence-magnitude curve was developed for each seismogeneic source. In addition, to consider the seismicity parameters utilized in Gutenberg-Richter magnitude frequency relations, a lower bound magnitude of M_w 4 is regarded for each fault (Abdalla and Al-Homoud 2004). Essential values that noticeable damages to the structures are occurred could be considered as the lower bound magnitude for PSHA regarding the

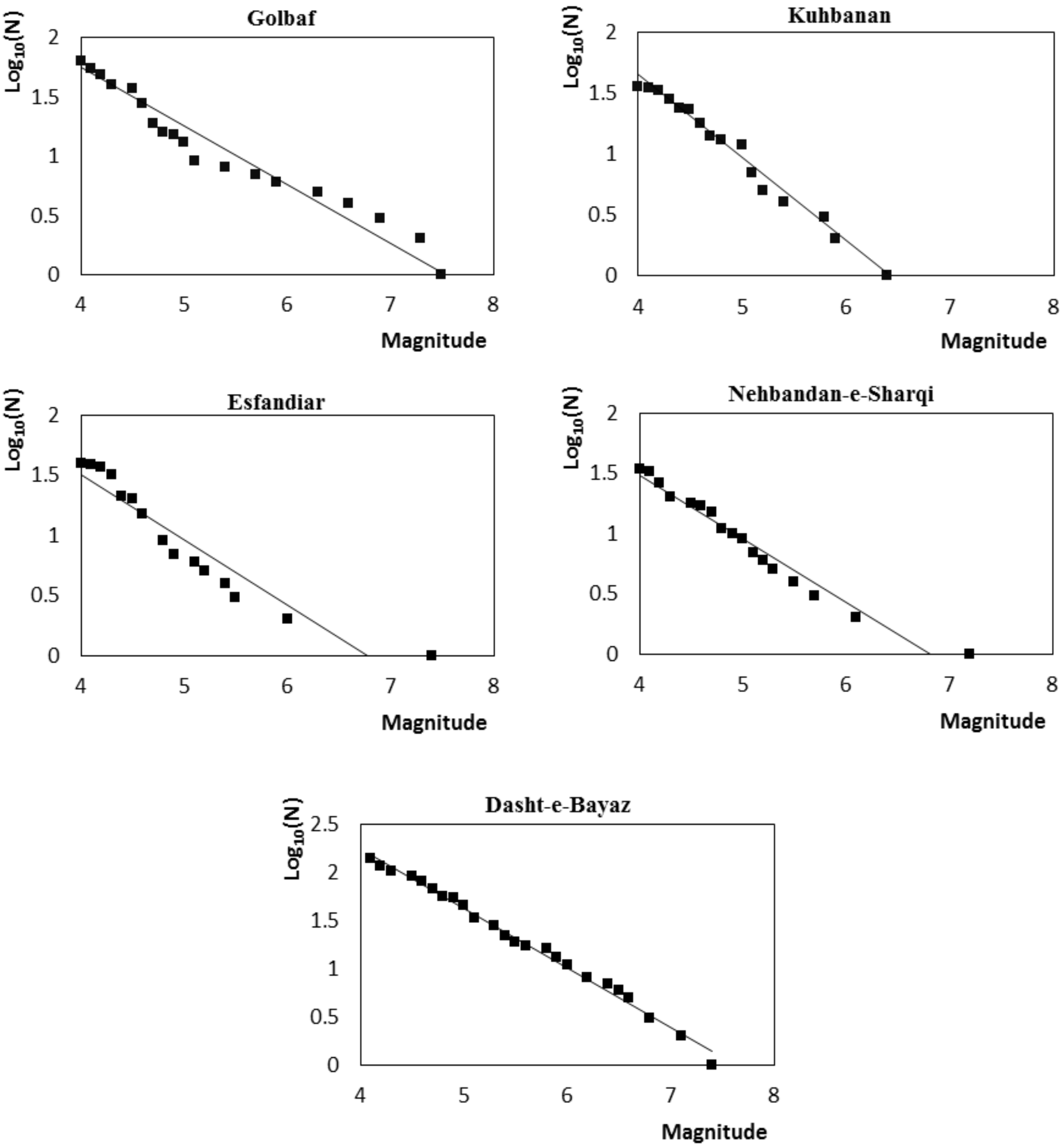

Fig. 3 G-R curves for the seismogenic sources

type of the structures in the area (Abdalla and Al-Homoud 2004). Additionally, the level of completeness of 4 is obtained for three different zones of Iran (Karimiparidari *et al.* 2013).

To produce G-R relationship, the scattered points were fitted with a line based on the least squares method. According to Eq. (4) has been established according to occurrence-magnitude graphs

$$\log(N) = a - bM \tag{4}$$

where *a* and *b* are constants, representative of the entire rate and potential of seismicity. Fig. 3 indicates the G-R relationship parameters for five seismogenic sources.

Regarding Gutenberg-Richter curves, the number of events with magnitude greater than M_w 5.5 is lesser than events with magnitude of M_w 5.5 or less. It seems that the G-R method is relatively accurate if we could use two or more lines in the curves. However, if the two line method is implemented, the second line probably has a lesser slope; results in much higher *N* values which misleadingly increase PGA. It is recommended that if the number of higher magnitude events is not enough; the one-line fitting method would be implemented to obtain higher accuracy in PGA estimation.

In some specific cases the truncation procedure could be avoided (McGuire 2004). In this regard, $M_{\min}$ is chosen on the basis of minimum magnitude that will cause damages or losses. Because of the weak constructed buildings in Iran (Maheri 2004), the magnitude of 4 is considered as the lower bound. It is worthy of notice that some earthquakes have occurred in Iran with approximate M_w of 4 which caused damages and heavy losses. In this regard, the Golbaf earthquake with magnitude of 4.6 occurred in 1999 made heavy damages to infrastructures located Kerman and Golbaf cities.

5.2 Effect of ground motion variability

The nature of earthquakes necessitates probabilistic approach to perform quantitative judgment. The highly variable earthquake occurrences have some consistent average behavior; therefore, our accurate assessments should be based on probabilistic terms (Kramer 1996, Baker 2008). As opposed to DSHA, probabilistic method considers the uncertainty and likelihood of an event as well as the ground shaking attenuation models. For each PGA regarding source-to-site distance and GMPEs, a magnitude was calculated. In general, the data source of Campbell GMPE is extracted from Western U.S. records, USSR, and Iran. The database consisted of 229 horizontal components of peak acceleration recorded from 27 earthquakes, including the 15 October 1979, Imperial Valley earthquake. Sadigh GMPE data source is accumulated from Western U.S. and worldwide for rock sites. The data source of Sadigh GMPE is obtained from worldwide records. The effect of distance on two implemented GMPEs could be observed in Fig. 4. By implementation of G-R law, the density of events' occurrence per area/length was evaluated.

Moreover, the effective life-span of structures assumed to be 50, 100, 200 and 500 years. The probability of exceedance could be assessed by the using Eqs. (5) and (6)

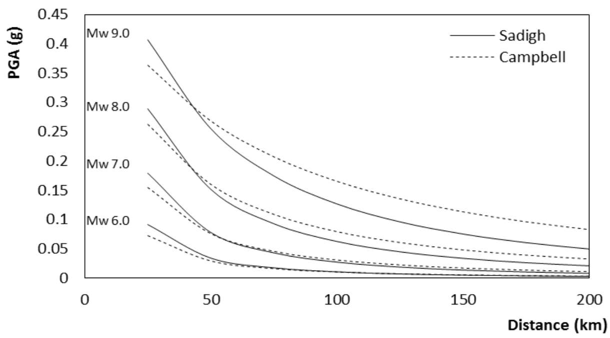

Fig. 4 Comparison of Sadigh and Campbell GMPEs

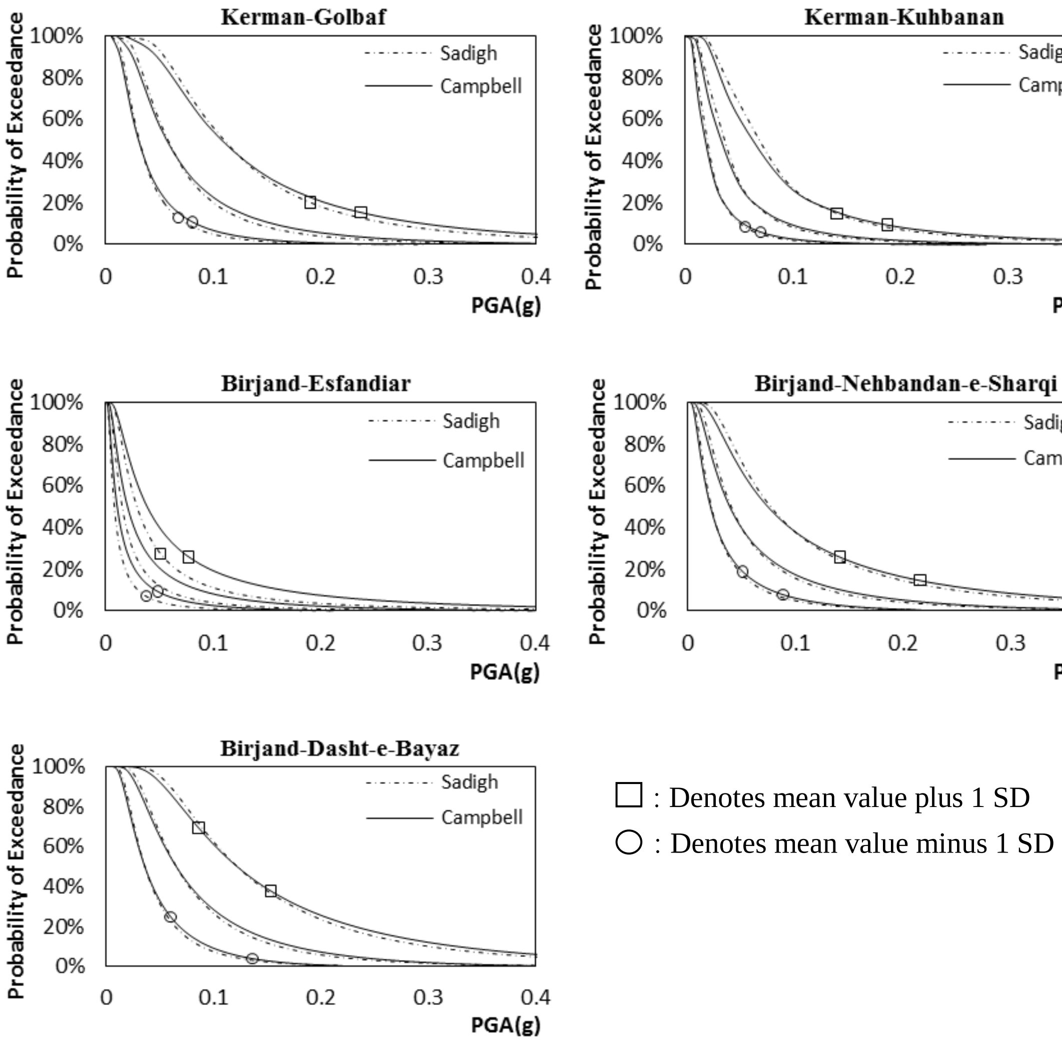

Fig. 5 PSHA curves for each individual sources based on Sadigh and Campbell GMPEs

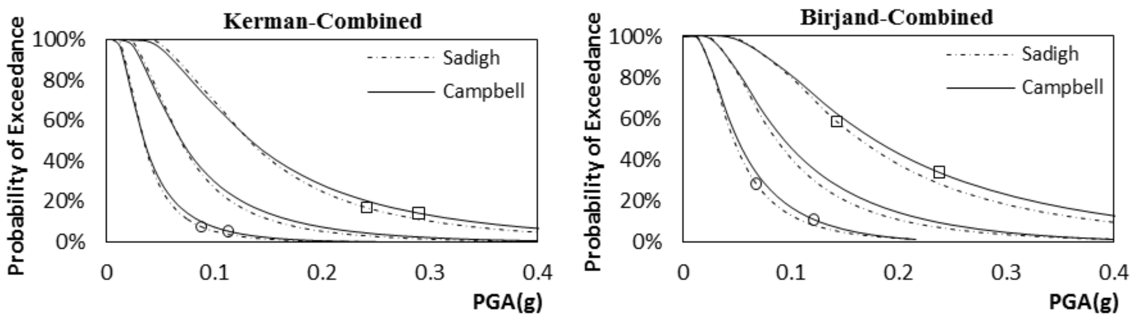

Fig. 6 PSHA curves of each city based on Sadigh and Campbell GMPEs

Table 4 Effect of different life-span for each fault regarding Sadigh GMPE

	Kuhbanan		**Golbaf**		**Esfandiar**		**Nehbandan-e-Sharqi**		**Dasht-e-Bayaz**	
Year \ POE	2%	10%	2%	10%	2%	10%	2%	10%	2%	10%
50	0.18	0.08	0.26	0.10	0.14	0.06	0.28	0.16	0.29	0.16
100	0.23	0.13	0.32	0.18	0.20	0.09	0.33	0.18	0.34	0.21
200	0.25	0.15	0.35	0.22	0.26	0.13	0.40	0.24	0.40	0.26
500	0.33	0.21	0.43	0.32	0.34	0.19	0.48	0.33	0.47	0.34

Table 5 Effect of different life-span for each fault regarding Campbell GMPE

	Kuhbanan		**Golbaf**		**Esfandiar**		**Nehbandan-e-Sharqi**		**Dasht-e-Bayaz**	
Year \ POE	2%	10%	2%	10%	2%	10%	2%	10%	2%	10%
50	0.18	0.09	0.28	0.15	0.21	0.09	0.30	0.17	0.30	0.18
100	0.23	0.13	0.35	0.20	0.27	0.13	0.35	0.20	0.35	0.23
200	0.28	0.18	0.42	0.26	0.33	0.19	0.39	0.26	0.39	0.28
500	0.35	0.24	0.45	0.33	0.39	0.27	0.44	0.34	0.43	0.35

Table 6 Effect of different life-span for studied sites

	Kerman				**Birjand**			
	Sadigh		Campbell		Sadigh		Campbell	
Year \ POE	2%	10%	2%	10%	2%	10%	2%	10%
50	0.28	0.16	0.31	0.18	0.35	0.21	0.36	0.23
100	0.33	0.20	0.35	0.23	0.39	0.26	0.41	0.29
200	0.38	0.25	0.40	0.28	0.45	0.32	0.43	0.34
500	0.45	0.33	0.48	0.36	0.50	0.41	0.46	0.40

- For Area Seismogenic Source: $$P(PGA \geq a) = 1 - e^{\sum N'(M) A T_L} \quad (5)$$
- For Line Seismogenic Source: $$P(PGA \geq a) = 1 - e^{\sum N'(M) L T_L} \quad (6)$$

where T_L is the assumed life-span of structures, $N'(M)$ is the density of events per unit area/length and A and L are the area and length of the fault, respectively.

Each seismogenic source was divided into distinctive parts, since the distance of each subpart from the site varies along the fault; this division enhances the accuracy of ultimate probable PGA, especially when the length/area of each fault is significant.

The obvious difference between DSHA and PSHA methods could have two main reasons. First, in the DSHA method, the Wells and Coppersmith formula was implemented for evaluation of surface magnitude; however, if the region is seismically active and the numbers of higher magnitude events would be significant, the higher POE may be expected for each PGA. Second, if a fault experiences an event with highly significant magnitude, the slope of G-R line would be reduced substantially leading to higher PGA estimation for an assumed POE, regarding events with higher magnitudes.

The effect of GMPE variability should be considered to improve the accuracy of POE calculation (Pavel *et al.* 2014). As illustrated in Fig. 5, the Campbell GMPE indicates higher values for PGAs more than 0.1 g considering a specified POE of the investigated regions. In addition, combined probabilistic curves indicated in Fig. 6 show higher values compared to probabilistic curves attributed to each fault due to the fact that for an assumed PGA, it is enough only one of the faults located in a region to be activated. It is clear that utilizing the combined PSHA curves would lead to more conservative results. It is important to note that the variability in the ground motions invalidates the procedure of obtaining the magnitude associated with each PGA and distance.

5.3 Effect of life-span

It is significant to note that most of the buildings in the studied regions are historical; therefore, having the ability to withstand earthquakes for longer periods of time is an essential factor for this area. In this regard, the effect of longer periods of life-span is evaluated in this part. By increasing the effective life-span of the structures, higher values for PGA are expected at a specified POE (Tables (4)-(6)).

6. Spectral acceleration

The spectral acceleration were provided regarding PGAs attributed to 2% and 10% levels of probability of exceedance based on results of Sadigh and Campbell GMPE hazard curves. The

Table 7 Spectral acceleration (cm/s^2) based on Sadigh GMPE regarding distance from each fault (km)

Fault Name	475 years				2475 years			
	50 km	100 km	150 km	200 km	50 km	100 km	150 km	200 km
Kuhbanan	327.0	153.5	91.4	60.0	115.8	54.4	32.4	21.2
Golbaf	243.1	114.2	68.0	44.6	777.9	365.3	217.4	142.6
Esfandiar	551.0	324.1	220.1	158.5	2079.4	1223.0	830.6	598.3
Nehbandan-e-Sharqi	36.4	17.1	10.2	6.7	81.6	38.1	22.8	15.0
Dasht-e-Bayaz	43.1	20.2	12.0	7.9	125.4	58.9	35.0	23.0

Table 8 Spectral acceleration (cm/s^2) based on Campbell GMPE regarding distance from each fault (km)

Fault Name	475 years				2475 years			
	50 km	100 km	150 km	200 km	50 km	100 km	150 km	200 km
Kuhbanan	105.8	49.7	29.6	19.4	278.7	130.9	77.9	51.1
Golbaf	198.5	93.2	55.5	36.4	583.6	274.0	163.1	107.0
Esfandiar	524.2	308.3	209.4	150.8	1881.8	1106.8	751.6	541.4
Nehbandan-e-Sharqi	36.4	17.1	10.2	6.7	81.6	38.3	22.8	15.0
Dasht-e-Bayaz	71.0	33.3	19.8	13.0	156.2	73.3	43.7	28.6

spectral acceleration curves were further developed by implementation of Sadeghi GMPE (2010). The natural frequency of structures is chosen to be 0.5 sec considering a number of buildings with mid-rise height in eastern parts of the Iran. The two well-known GMPEs for eastern part of the Iran were implemented to evaluate spectral acceleration response regarding distinctive source-to-site distance. Table 7 and Table 8 show the variability of spectral acceleration with source-to-site distance for each fault based on provided PGAs for two distinctive probabilities of exceedance. It has been observed that increasing source-to-site distance leads to spectral acceleration reduction with respect to each fault. In addition, the spectral acceleration rate of variation would increase if the source-to-site distance decreases.

7. Uniform hazard spectra (UHS)

Uniform hazard spectra estimated based on seismicity and seismotectonics of Kerman and Birjand cities. UHS curves generated for 2475-year and 475-year return periods are according to rock soil based on results of Sadigh and Campbell GMPE hazard curves. The UHS curves were further developed by implementation of Ghodrati Amiri *et al.* (2009) GMPE. The spectral accelerations are computed for T=0.1, 0.2, 0.3, 0.4, 0.5, 0.6, 0.7, 0.8, 0.9, 1, 1.25, 1.5, 2, 3, 4 sec. Figs. 9 and 10 indicate UHS curves for 2475-year return period according to Campbell and Sadigh GMPEs; it is important to note that structures with lower natural periods are the most vulnerable

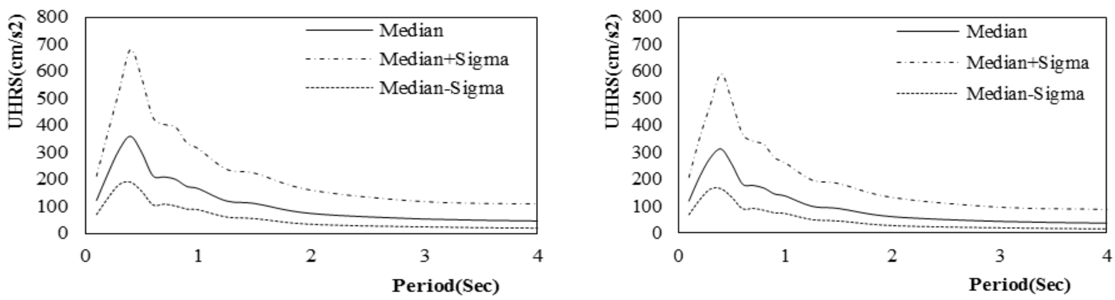

(a) based on Sadigh hazard curve (b) based on Campbell hazard curve

Fig. 9 UHS for Kerman with 2475-year return period

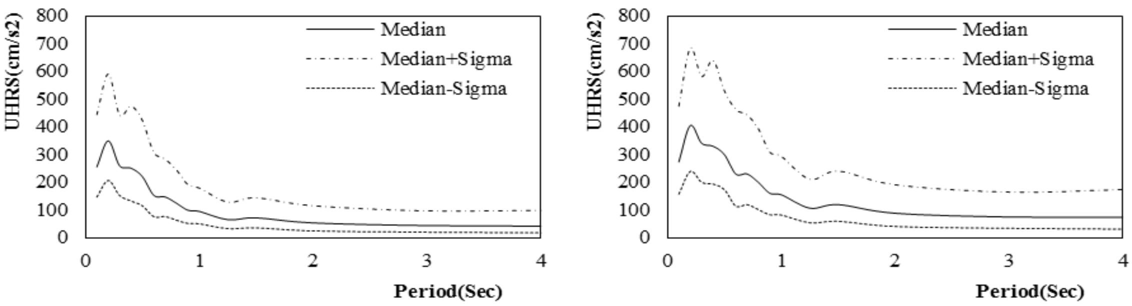

(a) based on Sadigh hazard curve (b) based on Campbell hazard curve

Fig. 10 UHS for Birjand with 2475-year return period

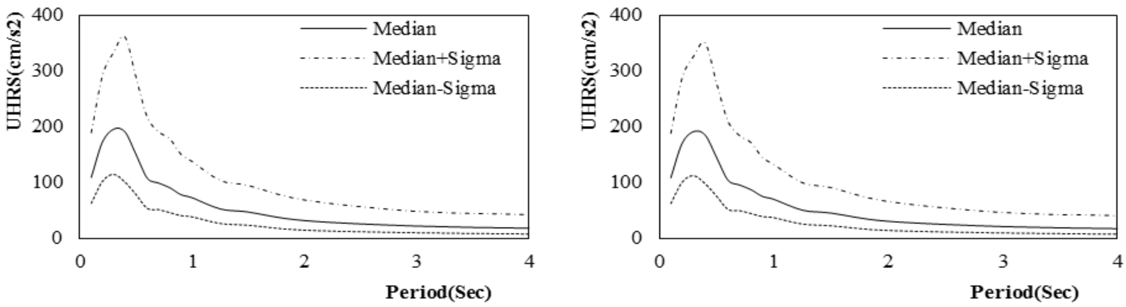

(a) based on Sadigh hazard curve (b) based on Campbell hazard curve

Fig. 11 UHS for Kerman with 475-year return period

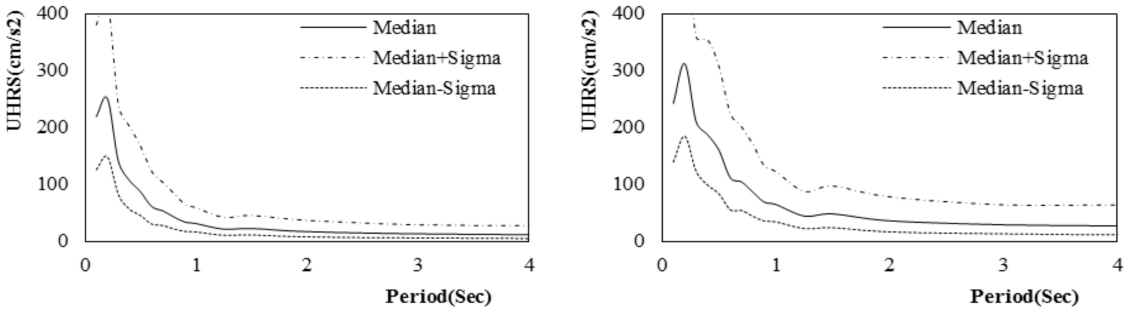

(a) based on Sadigh hazard curve (b) based on Campbell hazard curve

Fig. 12 UHS for Birjand with 475-year return period

ones in the studied areas. Additionally, it is observed that the highest spectral acceleration could be expected for structures with lower natural periods for Birjand area compared with that of the Kerman region. Furthermore, as for 475-year return period, similar trends to 2475-year return period are expected as indicated in Figs. 11 and 12.

8. Conclusions

This paper has investigated seismicity of Birjand and Kerman as two major cities of eastern of Iran based on probabilistic and deterministic approaches regarding different life-span of the structures. Response and hazard spectra curves are developed for these regions. The main results of this study are as follows:

In probabilistic approach, for the 2% POE, the probable PGA of Birjand and Kerman as for median PGA prediction are 0.36 g and 0.31 g, respectively. On the other hand, in deterministic method the estimated PGA for the stated cities is 0.35 g and 0.16 g, respectively. It has been observed that the PSHA approach may result in higher PGA values compared to DSHA; therefore, the latter method not necessarily leads to more conservative PGA calculations.

Application of different GMPEs might lead to a significant discrepancy in POE curves. In this regard, for the POE of 10%, the PGA is 0.18 g in the case of Campbell GMPE; however, this value has been estimated 0.16 g by Sadigh GMPE considering Kerman city. In addition, it has been observed that for POE of 2%, the PGAs for Kerman city according to Campbell and Sadigh GMPEs are 0.31 g and 0.28 g, respectively.

It has been observed that low height structures could be significantly vulnerable in eastern parts of the Iran, according to UHS curves. In addition, structures with the range 30 km or less source-to-site distance could be in danger of experiencing higher spectral acceleration according to spectral acceleration curves for eastern of Iran.

References

Abdollahzadeh, G., Sazjini, M., Shahaky, M., Zahedi Tajrishi, F. and Khanmohammadi, L. (2013), "Considering potential seismic sources in earthquake hazard assessment for Northern Iran", *J. Seismol.*, **18**(3), 357-369.

Abdalla, J.A. and Al-Homoud, A.S. (2004), "Seismic hazard assessment of United Arab Emirates and its surroundings", *J. Earthq. Eng.*, **8**(6), 817-837.

Alavi, A.H., Gandomi, A.H., Modaresnezhad, M. and Mousavi, M. (2011), "New ground-motion prediction equations using multi expression programing", *J. Earthq. Eng.*, **15**(4), 511-536.

Baker, J.W. (2008), *An Introduction to Probabilistic Seismic Hazard Analysis (PSHA)*, Version 1.3, Stanford University.

Bartels, S.A. and VanRooyen, M.J. (2012), "Medical complications associated with earthquakes", *Lancet*, **15**(4), 748-757.

Berberian, M. (1979), "Earthquake faulting and bedding thrust associated with the Tabas-e-Golshan (Iran) Earthquake of September 16, 1978", *Bul. Seismol. Soc. Am.*, **69**(6), 1861-1877.

Berberian, M. (1981), "Active faulting and tectonics of Iran", Eds. H.K. Gupta, F.M.D., Zagros-Hindu Kush-Himalaya Geodynamic Evolution: Washington D.C., American Geophysical Union, 33-69.

Berberian, M. (1982), "Aftershock tectonics of the 1978 Tabas-e-Golshan (Iran) earthquake sequence: a documented active 'thin- and thick-skinned tectonic' case", *Geophys. J.R. Astr. Soc.*, **68**(2), 499-530.

Berberian, M., Jackson, J.A., Ghorashi, M. and Kadjar, M.H. (1984), "Field and teleseismic observations of the 1981 Golbaf-Sirch earthquakes in SE Iran", *Geophys. J.R. Astr. Soc.*, **77**(3), 809-838.

Berberian, M. and Qorashi, M. (1994), "Coseismic fault-related folding during the South Golbaf earthquake of November 20, 1989, in south east Iran", *Geology*, **22**(6), 531-534.

Berberian, M., Jackson, J.A., Qorashi, M., Khatib, M.M., Priestly, K., Talebian, M. and Gafuri-Ashtiani, M. (1999), "The 1997 May 10 Zirkuh (Qa'enat) earthquake (M_w 7.2): faulting along the Sistan suture zone of eastern Iran", *Geophys. J. Int.*, **136**(3), 671-694.

Berberian, M., Jackson, J.A., Qorashi, M., Talebian, M. and Priestly, K. (2000), "The 1994 Sefidabeh earthquakes in eastern Iran: blind thrusting and bedding-plane slip on a growing anticline, and active tectonics of the Sistan suture zone", *Geophys. J. Int.*, **142**(2), 283-299.

Bilham, R. (2009), "The seismic future of cities", *Bul. Earthq. Eng.*, **7**(4), 839-887.

Campbell, K.W. (1981), "Near-source attenuation of peak horizontal acceleration", *Bul. Seism. Soc. Am.*, **71**(6), 2039-2070.

Cauzzi, C. and Faccioli, E. (2008), "Broadband (0.05 to 20 s) prediction of displacement response spectra based on worldwide digital records", *J. Seismol.*, **12**(4), 453-475.

Engdahl, E.R., Jackson, J.A., Myers, S.C., Bergman, E.A. and Priestly, K. (2006), "Relocation and assessment of seismicity in the Iran region", *Geophys. J. Int.*, **167**(2), 761-778.

Gardner, J.K. and Knopoff, L. (1974), "Is the sequence of earthquakes in Southern California, with aftershocks removed, Poissonian?", *Bul. Seismol. Soc. Am.*, **64**(5), 1363-1367.

Ghasemi, H., Zare, M., Fukushima, Y. and Koketsu, K. (2009), "An empirical spectral ground-motion model for Iran", *J. Seismol.*, **13**(4), 499-515.

Ghodrati Amiri, G., Motamed, R. and Rabet Es-Haghi, H. (2003), "Seismic hazard assessment of metropolitan Tehran, Iran", *J. Earthq. Eng.*, **7**(3), 347-372.

Ghodrati Amiri, G., Mahdavian, A. and Manouchehri Dana, F. (2007), "Attenuation relationships for Iran", *J. Earthq. Eng.*, **11**(4), 469-492.

Ghodrati Amiri, G., Khorasani, M., Mirza Hessabi, R. and Razavian Amrei, S.A. (2009), "Ground-motion prediction equations of spectral ordinates and arias intensity for Iran", *J. Earthq. Eng.*, **14**(1), 1-29.

Hosseinzadeh, M. (2008), "Uniform hazard spectra and simulated strong ground motion for Bam, Iran", *The 14th World Conference on Earthquake Engineering*, Beijing.

Karimiparidari, S., Zare, M., Memarian, H. and Kijko, A. (2013), "Iranian earthquake, a uniform catalog with moment magnitudes", *J. Seismol.*, **17**(3), 897-911.

Kijko, A. (2004), "Estimation of the maximum earthquake magnitude, $M_{\max}$", *Pure Appl. Geophys.*, **161**, 1655-1681.

Koreie, M.T. (2005), *Morphotectonic of Kuhbana Fault*, Geosciences No. 58 in Geological Survey of Iran.

Kramer, K.L. (1996), *Geotechnical Earthquake Engineering*, Prentice-Hall International Series in Civil Engineering and Engineering Mechanics, Upper Saddle River, New Jersey, USA.

McGuire, R.K. (2004), *Seismic Hazard and Risk Analysis*, Earthquake Engineering Research Institute, USA.

Maheri, M.R. (2004), "Performance of roofs and floor slabs during bam, earthquakes of 26 december 2003", *J. Seismol. Earthq. Eng.*, **6**(1), 123-131.

Mirzaei, N., Gao, M. and Chen, Y. (1999), "Delineation of potential seismic sources for seismic zoning of Iran", *J. Seismol.*, **3**(1), 17-30.

Motaghi, K. and Ghods, A. (2012), "Attenuation of ground-motion spectral amplitudes and its variations across the central Alborz mountains", *Bul. Seismol. Soc. Am.*, **102**(4), 1417-1428.

Mousavi, M., Ansari, A., Zafarani, H. and Azarbakht, A. (2012), "Selection of ground motion prediction models for seismic hazard analysis in the Zagros region, Iran", *J. Earthq. Eng.*, **16**(8), 1184-1207.

Pavel, F., Vacareanu, R., Arion, C. and Neagu, C. (2014), "On the variability of strong ground motions recorded from Vrancea earthquakes", *Earthq. Struct.*, **6**(1), 1-18.

Rahgozar, M.A., Ghodrati Amiri, G. and Saleh, M. (2012), "Probabilistic assessment of PGA and UHS for Bojnurd city, the capital of north Khorasan province, Iran", *J. Seismol. Earthq. Eng.*, **14**(1), 13-28.

Raschke, M. (2013), "Statistical modeling of ground motion relations for seismic hazard analysis", *J. Seismol.*, **17**(4), 1157-1182.

Regard, V., Hatzfeld, D., Molinaro, M., Aubourg, C., Bayer, R., Bellier, O., Yamini-Fard, F., Peyret, M. and Abbassi, M. (2010), "The transition between Makran subduction and the Zagros collision: recent advances in its structure and active deformation", *Geologic. Soc., London, Special Publications*, **330**(1), 43-64.

Reiter, L. (1990), *Earthquake Hazard Analysis-Issues and Insights*, Columbia University Press, New York, USA.

Sadeghi, H., Shooshtari, A. and Jaladat, M. (2010), "Prediction of horizontal response spectra of strong ground motions in Iran and its region", *Proceedings of the 9th U.S. National and 10th Canadian Conference on Earthquake Engineering*, Toronto.

Sadigh, K., Egan, J. and Youngs, R. (1986), "Specification of ground motion for seismic design of long period structures", *Earthq. Notes*, **57**(1), 13.

Saffari, H., Kuwatsa, Y., Takada, S. and Mahdavian, A. (2012), "Updated PGA, PGV, and spectral acceleration attenuation relations for Iran", *Earthq. Spec.*, **28**(1), 257-276.

Shafiei Bafti, A. (2009), "Tectonics movements of Kuhbanan fault system in Bahabad region, Central Iran", *Iran. J. Earth Sci.*, **1**(1), 92-98.

Shjoa-Taheri, J., Naserieh, S. and Hadi, G. (2010), "A test of the applicability of NGA models to the strong ground-motion data in the Iranian plateau", *J. Earthq. Eng.*, **14**(2), 278-292.

Shokri, M., Eskandari M. and Zia, M. (2011), *Primary report of Kahnouj earthquake 2011 Jun 15 (Kahnouj, Kerman)*, a report in Geological Survey of Iran.

Tavakoli, B. and Ghafory-Ashtiany, M. (1999), "Seismic hazard assessment of Iran", *Annali Di Geofisica*, **42**(6), 1013-1021.

Tavakoli, B. (2002), "Sensitivity of seismic hazard evaluations to uncertainties determined from seismic source characterization", *J. Seismol.*, **6**(4), 525-545.

Vacareanu, R., Demetriu, S., Lungu, D., Pavel, F., Arion, C., Iniancovici, M., Aldea, A. and Neagu, C. (2014), "Empirical ground motion model for Vrancea intermediate-depth seismic source", *Earthq. Struct.*, **6**(2), 141-161.

Walker, R.T., Jackson, J.A. and Baker, C. (2004a), "Active faulting and seismicity of the Dasht-e-Bayaz region, Eastern Iran", *Geophys. J. Int.*, **157**(1), 265-282.

Walker, R.T. and Jackson, J.A. (2004b), "Active tectonics and late Cenozoic strain distribution in central and eastern Iran", *Tectonics*, **23**(5).

Walker, R.T. and Khatib, M.M. (2006), "Active faulting in the Birjand region of NE Iran", *Tectonics*, **25**(4).

Walker, R.T., Gans, P., Allen, M.B., Jackson, J.A., Khatib, M., Marsh, N. and Zarrinkoub, M. (2009), "Late Cenozoic volcanism and rates of active faulting in eastern Iran", *Geophys. J. Int.*, **177**(2), 783-805.

Zare, M. and Hamzehloo, H. (2004), "A Study of the strong ground motions of 26 December 2003 Bam earthquake: Mw6.5", *J. Seismol. Earthq. Eng.*, **5**(4), 33-56.

Zare, M., Karimi-Paridari, S. and Sabzali, S. (2008), "Spectral attenuation of strong motions for near source data in Iran", *J. Seismol. Earthq. Eng.*, **10**(3), 147-152.

SA